Comparison between Breast MRI and Contrast-Enhanced Spectral Mammography

Authors' Contribution:
Study Design A
Data Collection B
Statistical Analysis C
Data Interpretation D
Manuscript Preparation E
Literature Search F
Funds Collection G

ABDEF 1 Elżbieta Łuczyńska
ACEF 1 Sylwia Heinze-Paluchowska
E 2 Edward Hendrick
BD 1 Sonia Dyczek
D 3 Janusz Ryś
F 4 Krzysztof Herman
F 5 Paweł Blecharz
F 6 Jerzy Jakubowicz

1 Department of Radiology, Cancer Centre and Institute of Oncology, Cracow, Poland
2 Department of Radiology, University of Colorado – Denver, School of Medicine, Aurora, CO, U.S.A.
3 Department of Pathology, Cancer Centre and Institute of Oncology, Cracow, Poland
4 Department of Surgical Oncology, Cancer Centre and Institute of Oncology, Cracow, Poland
5 Department of Oncological Gyneacology, Cancer Centre and Institute of Oncology, Cracow, Poland
6 Department of Radioteraphy, Cancer Centre and Institute of Oncology, Cracow, Poland

Corresponding Author: Sylwia Heinze-Paluchowska, e-mail: sylwia.heinze-paluchowska@ifj.edu.pl
Source of support: Departmental sources

Background: The main goal of this study was to compare contrast-enhanced spectral mammography (CESM) and breast magnetic resonance imaging (MRI) with histopathological results and to compare the sensitivity, accuracy, and positive and negative predictive values for both imaging modalities.

Material/Methods: After ethics approval, CESM and MRI examinations were performed in 102 patients who had suspicious lesions described in conventional mammography. All visible lesions were evaluated independently by 2 experienced radiologists using BI-RADS classifications (scale 1–5). Dimensions of lesions measured with each modality were compared to postoperative histopathology results.

Results: There were 102 patients entered into CESM/MRI studies and 118 lesions were identified by the combination of CESM and breast MRI. Histopathology confirmed that 81 of 118 lesions were malignant and 37 were benign. Of the 81 malignant lesions, 72 were invasive cancers and 9 were *in situ* cancers. Sensitivity was 100% with CESM and 93% with breast MRI. Accuracy was 79% with CESM and 73% with breast MRI. ROC curve areas based on BI-RADS were 0.83 for CESM and 0.84 for breast MRI. Lesion size estimates on CESM and breast MRI were similar, both slightly larger than those from histopathology.

Conclusions: Our results indicate that CESM has the potential to be a valuable diagnostic method that enables accurate detection of malignant breast lesions, has high negative predictive value, and a false-positive rate similar to that of breast MRI.

MeSH Keywords: Breast • Breast Neoplasms • Magnetic Resonance Imaging • Mammography

Full-text PDF: http://www.medscimonit.com/abstract/index/idArt/893018

📄 3452   🗏 5   📊 3   📚 36

Background

Breast cancer is the most common cancer in women worldwide, with 1.7 million women diagnosed with breast cancer in 2012 [1]. Between 2008 and 2012, worldwide breast cancer incidence rates have increased 20% and mortality rates have increased 14% [1]. It is important to find an accurate and cost-effective way to detect and diagnose early breast cancers in women across various ages, races, risk levels, economic levels, and geographic settings.

In the last few years, new methods have been developed using contrast media to detect breast cancers via tumor angiogenesis using dedicated breast computed tomography (CT) and breast magnetic resonance imaging (MRI) systems. Contrast-enhanced breast imaging techniques like CT and MRI are used for detection of angiogenesis by following contrast agent uptake in suspicious breast lesions [2–4]. Dedicated breast CT, however, is not yet widely available in developed or developing countries, and breast MRI is relatively expensive and available primarily in developed countries.

Contrast-enhanced breast MRI is currently the most sensitive technique to detect and stage breast cancer [5–8]. While appropriate indications for breast MRI are controversial, breast MRI is a viable option in developed countries for high-risk screening and a number of diagnostic indications, including detection and characterization of breast cancer, assessment of local extent of the disease, evaluation of treatment response, and guidance for biopsy and localization [9–11]. Breast MRI sensitivity values reported in high risk screening studies range from 77% to 100%, higher than those of other imaging modalities [12,13].

Interpretation of breast MRI exams has been aided by the American College of Radiology's breast-MRI-specific reporting and data system (BI-RADS) atlas and lexicon that illustrates and ranks the degree of suspicion of many of the morphological findings seen in contrast-enhanced breast MRI. The BI-RADS MRI lexicon also aids in the uniformity of reporting of breast MRI findings [14–18].

Despite its high sensitivity, breast MRI has been reported to have variable specificity, ranging from 81% to 99% in international multicenter studies of high risk women [19]. Other limitations of breast MRI include high equipment and examination costs, limited scanner availability, the inability to detect breast cancers based on calcifications, and variable sensitivity to *in situ* cancers [19–22].

Concurrent with the development of breast MRI and dedicated breast CT, the evolution of digital mammography has provided new opportunities for examination of the breast using high-resolution digital imaging combined with iodinated contrast agents. Two different approaches have been advanced. One, like breast MRI, is based on temporal subtraction of pre- from post-contrast images. In digital subtraction mammography (DSM), both pre- and post-contrast images are acquired during a single breast compression. DSM has the advantage of being able to acquire multiple post-contrast phases to study potential uptake and washout of contrast agent in suspicious lesions. DSM has the disadvantages of requiring long breast compression times (5–10 minutes) and as a result, patient discomfort, high likelihood of patient motion causing image misregistration, and the need for additional injections of contrast agent to acquire more than a single view of a single breast.

A second approach, the one pursued in this study, is dual-energy contrast-enhanced spectral mammography (CESM), which has the advantage of enabling acquisition of multiple views of both breasts after a single injection of contrast agent. In CESM, after administration of contrast agent each view consists of a rapidly acquired pair of low- and high-energy images. Low-energy images are normal mammograms with the x-ray beam spectrum set entirely below the k-edge of iodine (33.2 keV) by setting kVp to be less than 33 kV; high-energy images use 45–49 kVp and extra x-ray filtration to ensure that the x-ray beam spectrum is almost entirely above the k-edge of iodine. Low-energy images are acquired at the same dose as a normal digital mammogram, while high-energy images have only about 20% of the dose of a normal digital mammogram. A weighted subtraction of low- and high-energy images produces an image that maximizes the conspicuity of iodinated contrast agent in the breast while minimizing the structured noise of non-enhancing fibroglandular tissue, thus revealing lesions with higher neovascularity and extracellular leakage of contrast agent. The high spatial resolution of the digital detector reveals lesion details with approximately 10 times the spatial resolution of breast MRI.

The feasibility of CESM was demonstrated in 2003 by Lewin et al. using a prototype system. In a group of 26 subjects with mammographic or clinical findings warranting biopsy, 13 of which were invasive cancers, CESM showed strong enhancement in 11 cancers, moderate enhancement in 1 and weak enhancement in the other [23]. A larger clinical study by Dromain et al. that included 80 breast cancers showed that digital mammography plus CESM had higher sensitivity and superior receiver operating characteristic (ROC) curve areas than mammography alone or mammography plus ultrasound [24]. A multireader study using the same dataset showed that CESM added to mammography and ultrasound had significantly higher ROC curve areas than mammography and ultrasound [25].

The aim of this study was to see whether CESM is as effective as breast MRI in detecting and showing the full extent of

breast cancer – a question raised by Thibault et al. [26] and also addressed by 2 other recent papers, discussed later [27,28].

Material and Methods

Patients included in the study

The study was approved by an ethics committee and all enrolled patients provided written informed consent. CESM and MRI examinations, followed by histopathology verification, were performed between July 2012 and January 2013 in 102 patients who had suspicious lesions described in conventional mammography. Before the examinations, the level of urea in the blood, creatinine, and estimated glomerular filtration rate (eGFR) were determined. Exclusion criteria were an eGFR less than 30 mL/min, allergic reaction to iodinated or gadolinium-based contrast agents, claustrophobia, implanted pacemakers or metallic implants.

All patients were examined with CESM first, followed by breast MRI 1–7 days after CESM. In pre-menopausal women, the breast MRI exam was performed between the 5th and 12th day after the start of the menstrual cycle [29,30].

All visible lesions were evaluated by 2 experienced radiologists with 15 years of interpretation experience in mammography, 2 years in CESM, and 3 years in breast MRI (the evaluation was blinded, radiologists interpreted each modality independently, each assessing a similar number of MRI and CESM exams).

Digital Mammography (MG)

Conventional digital mammography was usually performed outside our hospital – all mammograms were evaluated retrospectively before the following examination by 1 of the 2 radiologists interpreting CESM and breast MRI.

Contrast Enhanced Digital Mammography (CESM)

All CESM exams were performed with a digital mammography device developed by GE Healthcare allowing dual-energy CESM acquisitions (SenoBright®). It consists of a full-field digital mammography system (Senographe Essential) using a flat panel detector with a cesium iodide (CsI) absorber, field size 24×31 cm, del pitch of 100 µm, image matrix size 2394×3062, and specific software and hardware adaptations for acquisition and processing of dual-energy images [31].

For the exam itself, a mammography technologist prepared patients by explaining the steps of the procedure and ensuring that the patient had no contraindications to iodine contrast. A nurse prepared patients for intravenous injection and placed a catheter into the antecubital vein of the arm contralateral to the breast of concern. A single-shot intravenous injection of 1.5 ml/kg of body mass of non-ionic contrast agent (Iopromide 370) was then performed, using a power injector (Covidien, Optistar™ Elite Injector) at rate of 3 ml/s with a bolus chaser of 30 ml of saline.

After a 2-minute delay, the mammography technologist positioned the patient and compressed the breast as for a conventional mammography exam mediolateral oblique (MLO) view. The breast without a suspected lesion was imaged first, followed by the breast with the suspected lesion, to increase the likelihood of contrast uptake in the breast of interest. For each breast, the MLO view was collected first, followed 1 minute later by the craniocaudal (CC) view. The CESM mode automatically collected 2 images in each view orientation: a low-energy acquisition at 26–30 kVp and a high-energy acquisition at 45–49 kVp, with kVp settings within those ranges depending on breast thickness and density. Low- and high-energy images were typically acquired within 1 second (s) of one another, with a maximum time separation of 3 s. For each high-energy acquisition, the SenoBright® application used a proprietary multi-layer x-ray filter to shape the resulting spectrum to maximize x-ray absorption by iodine. For each low- and high-energy pair, a weighted subtraction was performed automatically, generating an image that maximized the conspicuity of iodine contrast agent uptake [32].

Compression time for each view (i.e., low-energy, high-energy pair) was a maximum of 15 s. Total duration of the exam was no longer than 10 minutes. Both low-energy and weighted subtraction images in each view were immediately transferred to the workstation for radiologist viewing. A mammography workstation (GE's IDI Mammography Diagnostic Workstation) was used for viewing of processed images interpreted with knowledge of clinical history, with previous findings from mammography and US.

The total X-ray dose delivered to the patient for a pair of low- and high -energy images ranged between 0.7 and 3.6 milligray (mGy) depending on breast thickness and tissue composition. This dose level corresponds to about 1.2 times the dose delivered for a standard digital mammogram in "contrast" automatic optimization of parameters (AOP) mode on the Senographe Essential system. The average glandular dose (AGD) for the low-energy image was equal to that of a conventional mammogram, while the high-energy image had approximately 20% the dose of a conventional mammogram in AOP contrast mode.

After the CESM examination, patients were observed for 30 minutes to confirm that they had no allergic reaction to iodinated contrast agent.

MRI Protocol

All contrast-enhanced MRI examinations were performed with a 1.5T Avanto MRI system (Siemens, Erlangen, Germany). All patients underwent MRI examinations in the prone position using parallel imaging with an acceleration factor of 2.0. A dedicated 4-channel (Siemens) breast coil was used with the following acquisition protocol: T1-weighted turbo spin-echo (TSE) sequence, echo-planar diffusion-weighted imaging with apparent diffusion coefficient (DWI/ADC), T2-weighted TSE, and T2-weighted TSE with fat saturation (SPAIR) in the transverse plane. A 3D FLASH T1-weighted gradient-echo dynamic sequence with fat saturation (SPAIR) was performed before the administration of contrast agent, followed by 8 repetitions of the same sequence with a 20 s delay after starting the contrast injection (TR 5.16 ms, TE 2.38 ms, flip angle 10°; base resolution 384, phase resolution 75%, slice resolution 75%; FOV read 400 mm, FOV phase 59.4% with anterior-posterior phase encoding direction and voxel size 1.4×1.0×1.1 mm). Duration of each post-contrast acquisition was about 1 minute, depending on breast size. Post-contrast dynamic MR images were acquired after administration of 0.1 mmol/kg of body mass of gadolinium contrast agent (gadobutrol; 604.72 mg/ml) through a cannula positioned in an antecubital vein. Contrast medium was injected with the use of a power injector (Medrad) at a rate of 2 mL/s and was followed by administration of 20 mL of saline at the same rate.

MR images were processed by Brevis software (Siemens), and subtraction images, signal intensity-time curves (mean curves), and angiogenesis maps were obtained. Acquired images were transferred to a workstation (LEONARDO and SyngoVia, Siemens) for analysis and were interpreted with knowledge of clinical history and previous findings from mammography and US.

Evaluation of CESM and MRI

CESM was assessed using a BI-RADS-like classification (scale 1–5) [33].

The evaluation forms for MG and CESM included as appropriate the following data for each enhancing lesion found by the readers:
1. Lesion location (quadrant).
2. Degree of enhancement (none, slightly, medium, high).
3. Enhancement pattern:
   a. non-mass-like enhancement with no focal findings (linear, ductal, segmental, regional);
   b. focal enhancement (form, margin, and distribution according to BI-RADS) [33].

The MR imaging level of suspicion for the presence of malignant lesions was assigned a score from 1 to 5 using the MRI BI-RADS scale for suspicion of malignancy [14,16,17]. For both CESM and MRI interpretations, lesions receiving a BI-RADS score of 4 or higher were considered positive for cancer. Lesion size in both modalities was measured in 2D images. To account for geometric magnification of lesion size in CESM images, we corrected lesion sizes back to the mid-plane of the breast by multiplying lesion size at the image receptor by 0.94.

Statistical analysis

To compare MRI and CESM findings, receiver operating characteristic (ROC) per lesion analysis was performed, ROC curves were drawn, and the areas under full ROC curves (AUC) were compared using a Z-test. Sensitivity, specificity, accuracy, as well as positive and negative predictive values, were evaluated using BI-RADS scores ≥4 as positive assessments. Results were compared using McNamara's test corrected for continuity. Lesion size comparison was analyzed using a Student t-test for dependent variables, with alpha significance level defined as 0.05. Calculations were performed using STATISTICA 10.0 (StatSoft, Cracow, Poland) software.

Results

There were 102 consecutive patients who received paired CESM and MRI studies and 118 lesions were visualized by the combination of the 2 methods. Histopathological studies confirmed that 81 of the 118 lesions (69%) were malignant,
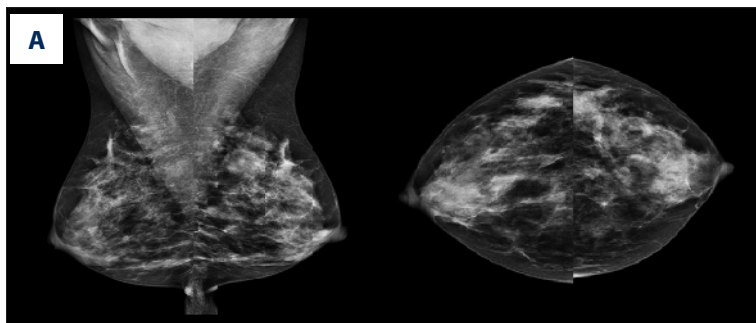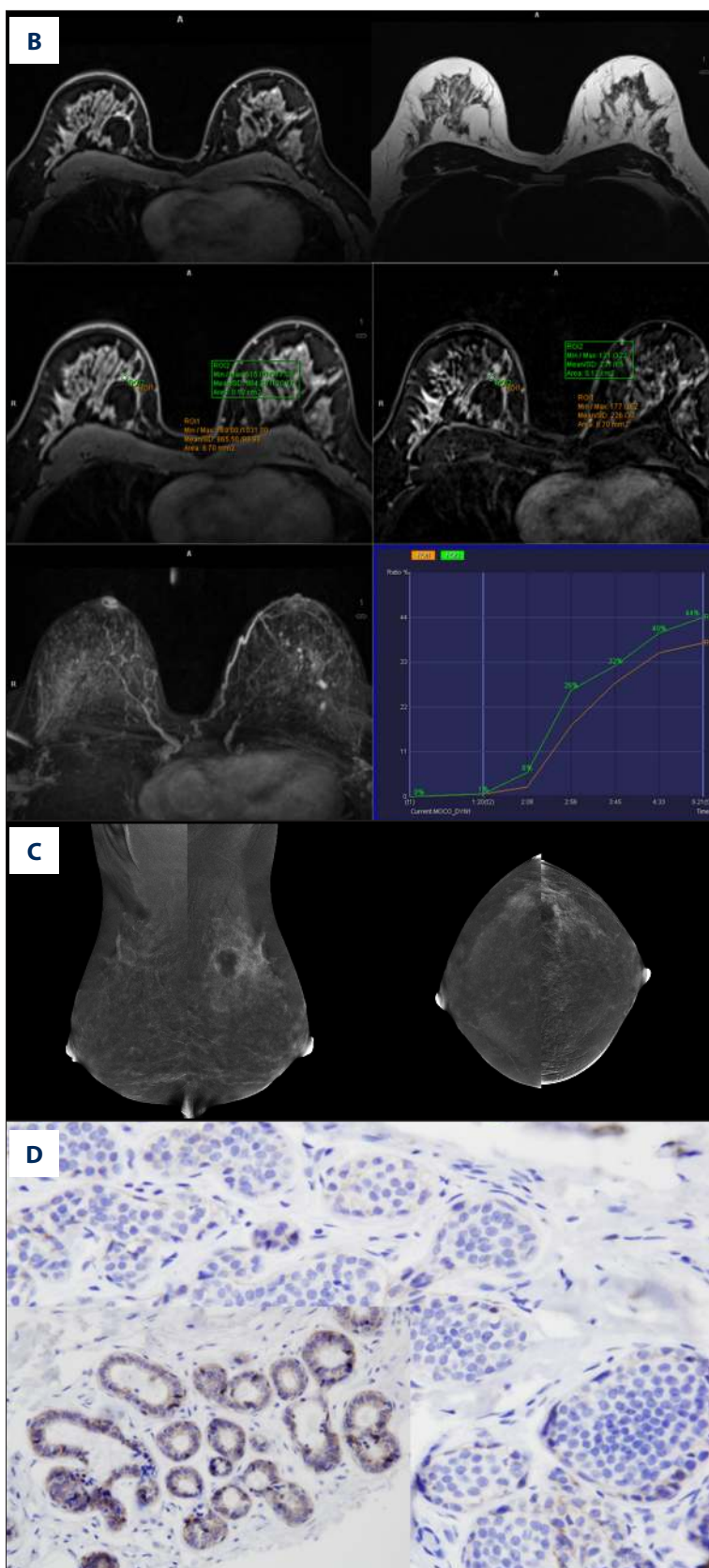
Figure 1. Breast images of a 51-year-old patient (**A**) initial digital mammography; (**B**) breast MRI – T1 and T2 weighted images, contrast enhanced T1 dynamic images with fat saturation and subtraction image 5 minutes after contrast injection (a cyst visible in T1 and T2 weighted images, no other focal lesions determined, small foci of contrast enhancement visible on the cyst wall, although the shape of the enhancement curve is non-characteristic – considering all the features of the lesion determined in MRI examination, the lesion was interpreted to be benign BI-RADS 2); (**C**) the CESM images with area of contrast enhancement near the cyst in the left breast (BI-RADS 4); (**D**) Histopathology – Atypical lobular hyperplasia/LCIS.

Table 1. Distribution of benign and malignant lesions in the study cohort.

Lesion	Cancer	Q-ty	Percent [%]
Infiltrating cancer	Invasive ductal carcinoma	58	49
	Invasive lobular carcinoma	5	4
	Apocrine carcinoma	1	1
	Papillary and micropapillary carcinoma	2	2
	Tubular carcinoma	1	1
	Mixed cases	5	4
Non-infiltrating cancer	Ductal carcinoma *in situ*	8	7
	Lobular carcinoma *in situ*	1	1
Benign lesions	Fibroadenoma	14	12
	Radial scar	4	3
	Intraductal papilloma	3	2
	Atypical ductal hyperplasia	1	1
	Inflammation	1	1
	Fibrosclerosis and fibrocystic lesions	14	12

Table 2. Distribution of lesions visible in MRI and CESM.

Number of lesions per patient	Lesion	Number of lesions	MRI – no enhancement	MRI – enhancement	CESM – no enhancement	CESM – enhancement
1	Benign	29	4	25	12	17
	Cancer	59	4	55	0	59
2	Benign	8	1	7	0	8
	Cancer	16	1	15	0	16
3	Benign	–	–	–	–	–
	Cancer	6	1	5	0	6
Total		**118**	**11**	**107**	**12**	**106**

Table 3. Sensitivity, accuracy, PPV and NPV according to BI-RADS assessment. Brackets indicate 95% confidence intervals. P-values assess the significance of differences between MRI and CESM by variable.

	Sensitivity	Accuracy	PPV	NPV
MRI	93%	73%	74%	65%
	[85%; 97%]	[64%; 81%]	[65%; 82%]	[38%; 86%]
CESM	100%	79%	77%	100%
	[96%; 100%]	[69%; 86%]	[67%; 84%]	[74%; 100%]
p value	0.04	0.29	0.72	<0.001

37 (31%) were benign (Figure 1). Of the 81 malignant lesions, 72 were invasive cancers and 9 were non-invasive cancers, as shown in Table 1. In 88 patients (86%) single breast lesions were detected, while in 12 patients (12%) 2 lesions were diagnosed, and in 2 patients (2%) 3 lesions were found.
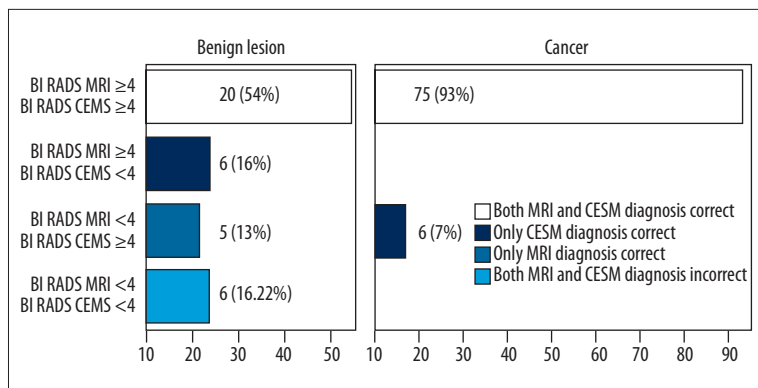
Figure 2. Comparison of BI-RADS in MRI and CESM. BI-RADS diagnosis based on MRI and CESM were consistent and correct in 93% of detected and histopathology-proven cancers. The remaining 7% of the observed cancers were properly diagnosed on CESM and mistakenly assessed on MRI. The classification was incorrect for both techniques in 54% of benign lesions. Among benign lesions, MRI incorrectly classified 70% as BI-RADS 4 or greater, while CESM incorrectly classified 68% as BI-RADS 4 or greater. Lesions that proved to be benign on histopathological examination were correct and consistent in 16%.

CESM found 106 lesions in 90 women. 72 lesions (68%) were invasive cancers, 9 lesions (8%) were non-invasive cancers, and 25 lesions (24%) were benign. In 76 women, single lesions were visible (59 malignant lesions and 17 benign lesions by histopathological verification). Twelve patients each had 2 contrast-enhanced breast lesions (16 malignant, 8 benign). In 2 patients, 3 contrast enhancement areas were visible and all of them were verified as malignant. 12 patients had no contrast enhancement by CESM (although suspicious lesions were visible in conventional mammography) and all lesions not diagnosed by CESM were benign.

MRI found 107 lesions in 94 women. 68 lesions (64%) were invasive cancers, 7 lesions (7%) were non-invasive cancers, and 32 lesions (30%) were benign. 11 lesions were undetected by MRI: 5 were benign, 4 were invasive cancers, and 2 were non-invasive cancers by histopathology. The 3 benign lesions undetected by MRI also were undetected by CESM. The described distribution of lesions is presented in Table 2.

CESM and MRI – BI-RADS Classification

On CESM, all 12 lesions classified as BI-RADS 1 proved to be benign on histopathology. Of 29 lesions classified as BI-RADS 4 on CESM, 13 (45%) were cancers. Of 77 lesions classified as BI-RADS 5 on CESM, 68 (88%) proved to be cancers on

histopathology. CESM had a sensitivity of 100%, an accuracy of 79%, a PPV of 77%, and an NPV of 100% (Table 3).

On MRI, of 11 lesions classified as BI-RADS 1, 6 (55%) were cancers on histopathology. Of 6 lesions classified as BI-RADS 2 on MRI, all proved to be benign. Of 40 lesions classified as BI-RADS 4 on MRI, 16 (40%) of them were cancers. Of 61 lesions categorized as BI-RADS 5 on MRI, 59 (97%) proved to be cancer (Figure 2).

Breast MRI had a sensitivity of 93%, an accuracy of 73%, a PPV of 74%, and an NPV of 65%. Sensitivity, accuracy, PPV and NPV of CESM and breast MRI, along with 95% confidence intervals, are summarized in Table 3. Sensitivity and negative predictive value were significantly better with CESM than with breast MRI (p values for significance of differences were 0.04 and <0.001, respectively).

Table 4 presents the correlation between lesions detected on MRI and CESM according to BI-RADS and lesion histopathology.

ROC analysis

The ROC curves based on BI-RADS classifications for MRI and CESM (Figure 3) are located a similar distance to the upper

Table 4. Correlation of CESM and MRI BI-RADS scores with histopathology. No lesions were scored as a BI-RADS 2 or 3 with CESM or BI-RADS 3 with MRI.

CESM – BI-RADS	Lesion	MRI – BI-RADS			
		1	2	4	5
1	Benign	3	3	6	0
	Cancer	–	–	–	–
4	Benign	2	3	10	1
	Cancer	2	0	7	4
5	Benign	0	0	8	1
	Cancer	4	0	9	55

This work is licensed under a Creative Commons
Attribution-NonCommercial-NoDerivs 3.0 Unported License

1364

Indexed in: [Current Contents/Clinical Medicine] [SCI Expanded] [ISI Alerting System]
[ISI Journals Master List] [Index Medicus/MEDLINE] [EMBASE/Excerpta Medica]
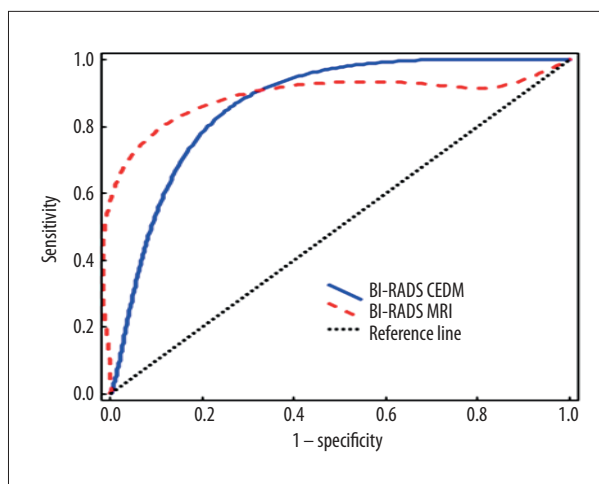[Chemical Abstracts/CAS] [Index Copernicus]

Figure 3. Comparison of ROC curves for CESM (blue line) and MRI (dashed red line) based on BI-RADS scores. Dotted reference line represents the ROC curve for a random distribution of cases with negative and positive test results.

left-hand corner of the graph, demonstrating their similar diagnostic performance (Figure 3).

ROC curve areas were comparable: AUC was 0.83 for CESM and 0.84 for MRI, with a p-value for the difference of 0.79 (Table 5).

Size estimation

Lesion sizes determined with CESM and breast MRI were similar, but were larger than those from histopathological examination (p<0.01). CESM overestimated average lesion size by 1.7 mm, while breast MRI overestimated average lesion size by 1.8 mm.

Discussion

At present, breast MRI is the most sensitive imaging technique for breast cancer detection and the most accurate for assessment of extent of disease. Breast MRI often is not available to women, however, due to lack of the technology or inadequate health insurance coverage. Moreover, the quality of breast MRI varies significantly across practices. The present study suggests that, like breast MRI, CESM could be of particular value for detection and assessment of extent of breast cancer. Our study found that CESM detected multifocal breast cancers in all cases studied and allowed reasonably accurate estimation of lesion size.

The dual-energy CESM technique offers the possibility of imaging both breasts in multiple views (CC and MLO) after a single injection of contrast agent. Like breast MRI, processed CESM images are sensitive to lesions revealed by contrast agent uptake. Beyond breast MRI, low-energy CESM images are sensitive to lesions revealed by the presence of calcification groups. The CESM exam takes less time than a breast MRI examination, where the patient must lie still in the prone position for a half-hour or longer during image acquisition. Moreover, CESM images are easy to interpret by radiologists familiar with standard mammography.

Mammography is the only breast imaging examination shown to reduce breast cancer mortality, with a population-based sensitivity of 75% to 80%. Sensitivity of mammography in high-risk women with dense breasts is only in the range of 50% [34].

The results of this study show that diagnoses based on CESM are slightly more reliable than those based on breast MRI. The sensitivity of CESM examination was 100%, higher than the 93% sensitivity of breast MRI (p≤0.04). The accuracy of the CESM exam was 79%, also higher than that of breast MRI (73%), but this difference was not statistically significant. PPV was 77% with CESM and 74% for breast MRI. NPV was 100% for CESM and only 65% for breast MRI (p<0.001).

Since CESM was only recently introduced into diagnostic use, there are only a few articles about it in the literature. Reported sensitivity values of CESM range between 63.5% and 93% [35]. Reported sensitivity values for MRI range from 77% to 100% [12,13]. To date, few papers have compared CESM to breast MRI in the same cohort [26,27]. In a study by Jochelson et al., all CESM examinations were performed in 1 imaging center, while MRI exams were performed in various institutions [27]. In that study, CESM had a lower sensitivity for depicting additional ipsilateral cancers than breast MRI, but the specificity of CESM was higher. An enhancing lesion seen on CESM was significantly more likely to be malignant than one seen on breast MRI, with a positive predictive value of 97% (64 of 66) for CESM and 85% (72 of 85) for breast MRI (p<0.01) [27]. In our study, 100% of cancers were identified as positive on CESM, while 93% were identified as positive on breast MRI.

Table 5. ROC analysis AUC values and 95% confidence intervals for MRI and CESM.

	MRI		CESM		AUC difference		
	Value	95% CI	Value	95% CI	Value	95% CI	p-value
ROC AUC	0.84	[0.76, 0.91]	0.83	[0.73, 0.92]	0.01	[0, 0.1]	0.79

While MRI permits detailed assessment of such parameters as contrast enhancement, mean curve shape, perfusion and diffusion of water molecules, its sensitivity appears to be lower than that of CESM. Fallenberg et al. showed an increase in lesion detection using CESM of 2.6% compared to MRI [28]. This paper confirms the findings of Fallenberg et al. and Jochelson et al., showing that CESM has a comparable or higher detection rate than breast MRI for primary breast cancers.

Unlike other CESM studies, we observed some differences in lesion dimensions between CESM and histopathology and between breast MRI and histopathology. These differences could be caused by breast compression during the MRI and CESM examinations. Overestimation of lesion sizes on acquired images had no influence on treatment because overestimation was small and safety margins were always included for surgical excision.

Our study has some limitations. All patients enrolled in the study were recalls from screening MG, which may have incurred some entry bias in favor of CESM compared to breast MRI. Another limitation of our study was that CESM is a novel technique and consequently does not yet have a dedicated BI-RADS lexicon and classification system; as a result, we adopted rules described by Diekmann [33]. A possible limitation of our ROC analysis could be relying on BI-RADS scores, which are non-linear in terms of cancer suspicion.

Conclusions

CESM is a new diagnostic method that enables accurate detection of malignant breast lesions, high negative predictive value, and a false-positive rate similar to that of breast MRI. However, further studies with a larger number of patients are necessary to confirm these conclusions.

References:

1. Siegel R, Naishadham D, Jemal A: Cancer statistics, 2013. Cancer J Clin, 2013; 63(1): 11–30

2. Kuhl CK: Concepts for differential diagnosis in breast MR imaging. Magn Reson Imaging Clin N Am, 2006; 14(3): 305–28

3. Kuhl C: The current status of breast MR imaging. Part I. Choice of technique, image interpretation, diagnostic accuracy, and transfer to clinical practice. Radiology, 2007; 244(2): 356–78

4. Prionas ND, Lindfors KK, Ray S et al: Contrast-enhanced dedicated breast CT: initial clinical experience. Radiology, 2010; 256(3): 714–23

5. Davis PL, McCarty KS: Sensitivity of enhanced MRI for the detection of breast cancer: new, multicentric, residual, and recurrent. Eur Radiol, 1997; 7(Suppl.5): 289–98

6. Benndorf M, Baltzer PAT, Vag T et al: Breast MRI as an adjunct to mammography: Does it really suffer from low specificity? A retrospective analysis stratified by mammographic BI-RADS classes. Acta Radiol, 2010; 51(7): 715–21

7. Swayampakula AK, Dillis C, Abraham J: Role of MRI in screening, diagnosis and management of breast cancer. Expert Rev. Anticancer Ther, 2008; 8(5): 811–17

8. Argus A, Mahoney MC: Clinical indications for breast MRI. Appl Radiol, 2010; 39(10): 10–19

9. ACR Practice Guideline for the Performance of Contrast-enhanced Magnetic Resonance Imaging of the Breast. Reston, VA: American College of Radiology; 2013

10. Mainiero MB, Lourenco A, Mahoney MC et al: ACR Appropriateness Criteria Breast Cancer Screening. J Am Coll Radiol, 2013; 10(1): 11–14

11. Wang Z, Li S, Wang L et al: Polyacrylamide hydrogel injection for breast augmentation: another injectable failure. Med Sci Monit, 2012; 18(6): CR399–408

12. Morris EA, Liberman L, Ballon DJ et al: MRI of occult breast carcinoma in a high-risk population. Am J Roentgenol, 2003; 181(3): 619–26

13. Berg WA: Rationale for a trial of screening breast ultrasound: American College of Radiology Imaging Network (ACRIN) 6666. Am J Roentgenol, 2003;180(5): 1225–28

14. Eberl MM, Fox CH, Edge SB et al: BI-RADS classification for management of abnormal mammograms. J Am Board Fam Med, 2006; 19(2): 161–64

15. Monticciolo DL, Caplan LS: The American College of Radiology's BI-RADS 3 Classification in a Nationwide Screening Program: current assessment and comparison with earlier use. Breast J, 2004; 10(2): 106–10

16. Liberman L, Menell JH: Breast imaging reporting and data system (BI-RADS). Radiol Clin North Am, 2002; 40(3): 409–30, v

17. Mahoney MC, Gatsonis C, Hanna L et al: Positive predictive value of BI-RADS MR imaging. Radiology, 2012; 264(1): 51–58

18. D'Orsi CJ, Sickles EA, Mendelson EB et al: ACR BI-RADS® Atlas, Breast Imaging Reporting and Data System. 5th ed. Reston, VA: American College of Radiology; 2013

19. Saslow D, Boetes C, Burke W et al: American Cancer Society guidelines for breast screening with MRI as an adjunct to mammography. Cancer J Clin, 2007; 57(2): 75–89. Erratum in: Cancer J Clin, 2007; 57(3): 185

20. Brennan M, Spillane A, Houssami N: The role of breast MRI in clinical practice. Aust Fam Physician, 2009; 38(7): 513–19

21. Lehman CD: Role of MRI in screening women at high risk for breast cancer. J Magn Reson Imaging, 2006; 98(5): 964–70

22. Misra S, Solomon NL, Moffat FL, Koniaris LG: Screening Criteria for Breast Cancer Adv Surg, 2010; 44: 87–100

23. Lewin JM, Isaacs PK, Vance V, Larke FJ: Dual-energy contrast-enhanced digital subtraction mammography: feasibility. Radiology, 2003; 229(1): 261–68

24. Dromain C, Thibault F, Muller S et al: Dual-energy contrast-enhanced digital mammography: initial clinical results. Eur Radiol, 2011; 21(3): 565–74

25. Dromain C, Thibault F, Diekmann F et al: Dual-energy contrast-enhanced digital mammography: initial clinical results of a multireader, multicase study. Breast Cancer Res, 2012; 14(3): R94

26. Thibault F, Balleyguier C, Tardivon A, Dromain C: Contrast enhanced spectral mammography: better than MRI? Eur J Radiol, 2012; 81(Suppl.1): S162–64

27. Jochelson MS, Dershaw DD, Sung JS et al: Bilateral contrast-enhanced dual-energy digital mammography: feasibility and comparison with conventional digital mammography and MR imaging in women with known breast carcinoma. Radiology, 2013; 266(3): 743–51

28. Fallenberg EM, Dromain C, Diekmann F et al: Contrast-enhanced spectral mammography versus MRI: Initial results in the detection of breast cancer and assessment of tumour size. Eur Radiol, 2014; 24(1): 256–64

29. Delille J-P, Slanetz PJ, Yeh ED et al: Physiologic changes in breast magnetic resonance imaging during the menstrual cycle: perfusion imaging, signal enhancement, and influence of the T1 relaxation time of breast tissue. Breast J, 2005; 11(4): 236–41

30. Ellis RL: Optimal timing of breast MRI examinations for premenopausal women who do not have a normal menstrual cycle. Am J Roentgenol, 2009; 193(6): 1738–40

31. Skarpathiotakis M, Yaffe MJ, Bloomquist AK et al: Development of contrast digital mammography. Dwyer SJ III, Schneider RH (eds.). Med Phys, 2002; 29(10): 2419–26

32. Puong S, Bouchevreau X, Patoureaux F et al: Dual-energy contrast enhanced digital mammography using a new approach for breast tissue canceling. Proc SPIE, 2007; 6510(0): 65102H

33. Diekmann F, Freyer M, Diekmann S et al: Evaluation of contrast-enhanced digital mammography. Eur J Radiol, 2011; 78(1): 112–21

34. Jochelson M: Advanced Imaging Techniques for the Detection of Breast Cancer. Am Soc Clin Oncol, 2012; 65–69

35. Rankin SC: MRI of the breast. Br J Radiol, 2000; 73(872): 806–18

36. Fallenberg EM, Dromain C, Diekmann F et al: Contrast-enhanced spectral mammography versus MRI: Initial results in the detection of breast cancer and assessment of tumour size. Eur Radiol, 2014; 24(1): 256–64